Nanoholes in metals with applications to sensors and spectroscopy

P. Marthandam

Department of Electrical and Computer Engineering,
University of Victoria, P.O. Box 3055,
Victoria, B.C., Canada, V8W 3P6
E-mail: pramodha@uvic.ca

A.G. Brolo*

Department of Chemistry,
University of Victoria, P.O. Box 3065,
Victoria, B.C., Canada, V8W 3V6
E-mail: agbrolo@uvic.ca

D. Sinton

Department of Mechanical Engineering,
University of Victoria,
P.O. Box 3055, Victoria, BC, Canada, V8W 3P6
E-mail: dsinton@me.uvic.ca

K.L. Kavanagh

Department of Physics,
Simon Fraser University, 8888 University Drive,
Burnaby, B.C., Canada, V5A 1S6
E-mail: kavanagh@sfu.ca

Matthew G. Moffitt

Department of Chemistry,
University of Victoria, P.O. Box 3065,
Victoria, B.C., Canada, V8W 3V6
E-mail: mmoffitt@uvic.ca

R. Gordon*

Department of Electrical and Computer Engineering,
University of Victoria, P.O. Box 3055,
Victoria, B.C., Canada, V8W 3P6
E-mail: rgordon@uvic.ca
*Corresponding authors

Abstract: In this paper, we review our experimental and theoretical investigations of nano-holes in metal films. Our first contribution to this field was to demonstrate experimentally that the shape of the holes in arrays could be used to influence the optical properties; in particular, we showed how to control the polarisation with elliptical nano-holes. A theory explaining this shape-effect was presented for a single rectangular hole. This theory agreed well with experimental findings. Furthermore, the separate contributions of the isolated hole and the lattice were shown experimentally and theoretically by varying the orientation and shape of the isolated holes. A new double-hole structure was presented to enable significantly enhanced local fields in the nano-holes, which has applications in non-linear optics and spectroscopy. Theory and experiments are presented for this double-hole structure, showing enhanced second-harmonic generation. We have used nano-hole arrays in surface plasmon resonance spectroscopy, surface-enhanced Raman spectroscopy and enhanced fluorescence. Along with those works, we present studies on the coupling between surface plasmons and quantum dots in nano-hole array samples. Finally, our work on integrating nano-hole samples into microfluidic devices for sensing applications is presented.

Keywords: surface plasmons; extraordinary transmission; nanoholes; sub-wavelength apertures; surface-enhanced Raman scattering; surface plasmon resonance.

Reference to this paper should be made as follows: Marthandam, P., Brolo, A.G., Sinton, D., Kavanagh, K.L., Moffitt, M.G. and Gordon, R. (2008) 'Nanoholes in metals with applications to sensors and spectroscopy', *Int. J. Nanotechnol.*, Vol. 5, Nos. 9/10/11/12, pp.1058–1081.

Biographical notes: Pramodha Marthandam received her Bachelors Degree in Electronics and Instrumentation Engineering from Anna University, India in 2005. She is a graduate student in the Department of Electrical and Computer Engineering at the University of Victoria, pursuing a Masters Degree. Her interests are in fabrication of nanostructures for optical applications.

Alexandre G. Brolo is an Associate Professor of Chemistry at the University of Victoria in Canada. He received his MSc and PhD in Chemistry from the University of Sao Paulo in Brazil and the University of Waterloo in Canada, respectively. His current interests are on the application of 'in situ' spectroscopic methods to study electrochemical systems, and on the development of substrates for enhanced spectroscopy, chemical sensing and nano-photonics.

David Sinton is currently an Assistant Professor in Mechanical Engineering at the University of Victoria, Canada. He started in 2003 following MASc studies at McGill University, and PhD studies at the University of Toronto, Canada. His research area is micro- and nano-fluidics, and his current interests involve the application of micro/nano transport and optical phenomena toward chemical analysis and energy conversion.

Karen L. Kavanagh is a Professor of Physics at Simon Fraser University, British Columbia. She obtained a BSc Degree in Chemical-Physics from Queen's University in 1978, and a PhD in Materials Science and Engineering from Cornell University in 1987. After post doctoral work at IBM and MIT she accepted a faculty position in the Electrical and Computer Engineering Department at UC San Diego until moving back to Canada in January 2000. Her main field of interest is electronic materials science, with current interests in nanophotonics, spintronics and nanostructural characterisation. She has

received an NSF Presidential Young Investigator Award and an NSERC University Faculty Award. She is the author of 80 journal papers and conference proceedings.

Matthew G. Moffitt obtained his PhD at McGill University under the supervision of Professor Adi Eisenberg and was an NSERC post-doctoral fellow in the group of Professor Mitch Winnik at the University of Toronto. He is currently an Assistant Professor in the Department of Chemistry at the University of Victoria. His research interests in physical polymer chemistry and materials target the application of spontaneous structure-forming processes in polymer systems (e.g., phase separation, dewetting, micellisation) for the self-assembly of metal and semiconducting nanoparticles within hybrid materials with structural hierarchy.

Reuven Gordon is an Associate Professor in Electrical and Computer Engineering at the University of Victoria, Canada, since 2002. He received his BASc in Engineering Science and MASc in Electrical Engineering from the University of Toronto, Canada, and PhD in Physics from the University of Cambridge, UK. He received the Canadian Advanced Technology Alliance award for best graduate student in Telecommunication Hardware (2001) and his work on the invention of transverse mode-locking in micro-cavity lasers was patented by Hitachi. His recent research contributions have been mainly in the area of nanophotonics.

1 Introduction

In 1998, Ebbesen and co-workers reported enhanced transmission through arrays of sub-wavelength holes (nano-holes) in metal films [1]. Peaks in the transmission spectra were observed, and the transmission efficiency was found to exceed unity when normalised to the hole-area. Enhanced transmission was reported in isolated apertures as well [2]. Since those discoveries [1,2], considerable research effort has been directed to the understanding of the physical mechanisms behind the enhanced optical transmission through sub-wavelength apertures in metal films. These efforts were driven by the potential of using these nano-holes in metal films in several applications, including optical filters [3], near-field spectroscopy [4], nano-imaging [5], non-linear optics [6] and sub-wavelength lithography [7].

The enhanced transmission was originally attributed to surface plasmon polaritons (SPPs) [1]. SPPs are electromagnetic waves that propagate along an interface between a metal and a dielectric [8]. The coupling between the SPPs and free-space light was considered to arise from the Bragg condition imposed by the periodicity of the array of nano-holes. The condition for surface plasmon resonance (SPR) by grating coupling is given by:

$$\lambda^{SP}(i,j) = p(i^2 + j^2)^{-1/2}\left(\frac{\varepsilon_d \varepsilon_m}{\varepsilon_d + \varepsilon_m}\right)^{1/2}. \tag{1}$$

The wavelength for coupling (λ^{SP}) is governed by the periodicity p of the array. ε_d is the relative permittivity of the dielectric, ε_m is the dielectric constant of the metal, and i and j are integers related to the scattering order of the grating [1,9]. The enhanced transmission

was observed for typical metals that support SPPs in the visible range, such as gold, silver and copper films. On the other hand, the phenomenon was not observed from nanostructures in materials that do not support SPPs, such as germanium films.

More recently, it has been suggested that SPPs do not play a causal role in the enhanced transmission [10–12]. Rather, it has been proposed that the observed resonances are essentially a diffraction phenomenon, of which SP waves are only one component [10]. In some cases, the SPPs can have a negative effect on transmission through sub-wavelength apertures [11]. A comprehensive model of diffractive evanescent waves has been compared with a variety of aperture structures [12]. These findings suggest that although SPPs may have an effect on enhanced transmission, they may not necessarily be causal to the phenomenon [10–12].

The shape of the nano-holes in the arrays was shown to have an influence on the polarisation of the transmitted light [13], as well as on the resonance peak wavelength [14,15]. Elliptical holes of increased ellipticity showed stronger polarisation selection [13]. The orientation of the elliptical holes within the lattice was also shown to determine the polarisation of the transmission [16]. For rectangular holes, the aspect ratio was found to influence both the transmission wavelength and polarisation properties [14,15]. This shape effect was also shown for randomly distributed rectangular apertures [14,15]. Measurements on a single rectangular hole showed that the cut-off wavelength and the normalised transmission increased as the length of the short edge of the hole were decreased [17]. Localised surface plasmons (LSPs) were used to explain this phenomenon, lending support to the theory that surface plasmons do in fact play a role in the enhanced transmission even through a single hole. Those findings all show that the shape of the individual nano-hole is crucial to determine its optical properties.

Single nano-holes and arrays of nano-holes in metal films may be exploited to increase the local field intensity. This effect leads to an enhancement in the fluorescence emission of molecules within the holes. Studies have been reported for enhanced fluorescence arising from a single rectangular aperture [18], single circular aperture [19], and arrays of circular apertures [20]. We have explored novel double-hole structures to create sharp apexes that increase the local field intensity, as demonstrated with non-linear optical measurements [21].

The sub-wavelength optical properties of nano-hole arrays can be harnessed for applications in spectroscopy and sensing. SPR has been exploited widely for the sensing of sub-monolayer amounts of bio-molecules, which has relevance for drug-development [22]. We were the first to use nano-hole arrays as SPR substrates for monolayer sensing. Surface-enhanced Raman scattering (SERS) is another chemical application that relies on local field enhancements from metal surfaces [4]. We have also demonstrated SERS from nano-hole arrays. Many other applications exist for nano-holes in metal films, such as optical filters [3] and second harmonic generation (SHG) [6,23].

In this paper, we will review our research into the development of nano-hole arrays for sensing and spectroscopy. Our contributions have been towards the understanding of the shape effect in nano-holes, including the dependence of the polarisation on the orientation of the nano-holes within the array. We also explored the effect of SPPs on the optical properties of nano-holes, and developed new configurations of nano-holes for enhanced spectroscopy, such as SERS. A chemical sensor based on an array of nano-holes was also developed and integrated into microfluidic devices. In Section 2, we summarise the shape effect on the transmission and optical properties of nano-holes. In Section 3, we describe enhanced transmission and second harmonic generation in

double nano-hole apexes. In Section 4, we summarise the results of nano-hole enhanced spectroscopy. In Section 5, we present some of our work on nano-hole based sensors. Although many groups have made valuable contributions to this field, we primarily highlight our direct contributions below.

2 Optical properties of shaped nano-holes

2.1 Elliptical nano-holes

In early numerical works on the enhanced transmission through nano-hole arrays in metal films, either circular or square holes were considered. In some cases, it was assumed that the basic transmission properties would not be influenced by the hole-shape [24]. Our studies of the transmission through elliptical holes in gold films were the first to show the impact of hole-shape on the transmission. In later works, more comprehensive studies of the shape effect in rectangular holes were presented, both for periodic and random arrays [14,15].

All nano-hole arrays that we investigated were created by focused ion beam (FIB) milling. A Ga^+ ion beam of 30 keV was used to mill a 100 nm thick gold film [13]. Each time, several calibration runs were carried out to determine the beam dwell time to mill through the gold. Stream files specifying the pixel coordinates and the corresponding burn time for milling were loaded into the user interface of the FIB station. For elliptical holes, astigmatic beams were used.

We explored the effect of changes in the shape (aspect ratio) and orientation of the nano-holes on both the transmission intensity and polarisation. Figure 1 shows the transmission spectra for two orthogonal linear polarisations of light through an array of elliptical nano-holes. The *p*-polarisation was defined along the [0, 1] direction of the array, which is perpendicular to the major axis of the ellipse, as shown in the inset of Figure 1. A clear reduction in the peak was observed as the polarisation was changed from *p*-polarisation to *s*-polarisation.

Figure 1 Transmission spectra through an array of elliptical nano-holes milled on a gold film. Aspect ratio 0.3. *p*-polarisation is parallel to [0, 1] direction. Reprinted with permission from [13]. Copyright 2004 American Physical Society

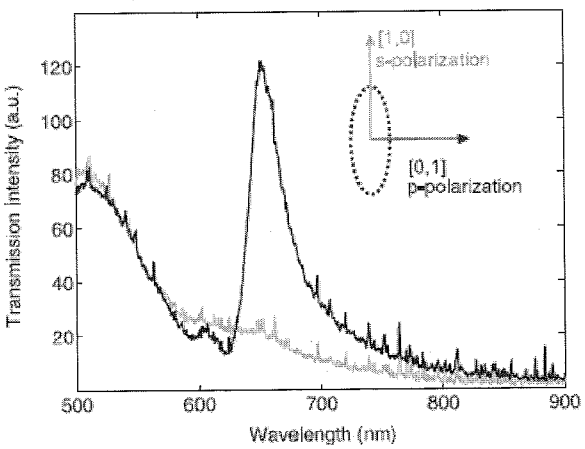

The orientation of the elliptical nano-holes was rotated relative to the lattice, and the transmission spectra of light polarised linearly along several directions between *s*- and *p*-polarisations were measured. It was found that the orientation of the electric field polarisation corresponding to the peak in transmission follows the orientation of the ellipse. This is partly because the SP modes propagate parallel to the electric field polarisation [8], and the Bragg resonance from the array is aligned with the optical polarisation. Thus, the transmission was enhanced for polarisation that is parallel to the direction in which the ellipse orientation allows for enhancement of SP mode coupling. A second reason for this polarisation dependence was later found when we compared double-hole and elliptical hole structures for different orientations, as will be discussed in Section 2.3. It was shown that the shape of each isolated hole also influences the transmission properties. Recent studies have used these results to create polarisation-tunable optical filters [3]. It was suggested that these could be used as colour filters for high definition television.

2.2 *Rectangular holes*

Following our first demonstration of how the hole-shape can be used to control the optical properties of the substrate, we investigated further the physical mechanisms behind the shape-effect. At this time, two other key experimental works had been published on rectangular holes, where it was shown that by decreasing the short-edge width of the rectangular hole, the wavelength of maximum transmission actually increased [14,17]. The first work considered periodic and random arrays of rectangular holes [14], whereas the second work considered an isolated rectangular hole [17]. In the isolated hole case, it was clear that this increased transmission effect originated from the shape of the single hole alone [17]. That effect was attributed to LSPs.

We made two main contributions to the understanding of the physics of this phenomenon. First we showed how the LSPs within the hole influence the cut-off wavelength and thereby permit longer wavelengths to transmit through the hole as the length of the short-edge is reduced for a rectangular hole in a real metal [25]. Second, we explained the origin of the peak in the transmission through the hole in terms of Fabry-Pérot (FP) resonances of the fundamental mode within the hole between the two surfaces of the metal film [26]. The findings of our theoretical works agreed well with the results of experiments on rectangular nano-holes as reported in [14] and [17].

2.2.1 *Increased cut-off wavelengths for transmission*

For a rectangular waveguide made of a perfect electric conductor (PEC), the electric field penetration into the metal is expected to be zero. The cut-off wavelength of the lowest order mode is given by:

$$\lambda = 2l \tag{2}$$

where l is the long edge of the rectangle.

When a waveguide mode of a single rectangular aperture was studied experimentally for a real metal, it was found that the cut-off wavelength for transmission increased with the aspect ratio [17]. We studied this problem theoretically for nano-holes on silver using an effective-index method, in conjunction with rigorous electromagnetic computations [25]. It was found that the increased cut-off wavelengths were due to two separate

physical effects: the penetration of electric field into the metal, which does not happen for a PEC, and the coupling of SP modes on the top and bottom edges inside the hole.

First, the penetration of the electric field into the metal allows for a longer wavelength inside the hole and thereby increases the cut-off wavelength. The cut-off wavelength for a rectangular aperture in a real metal is given by [25]:

$$\lambda_{\text{cut-off}} = \frac{\pi l \sqrt{\varepsilon_d}}{\arctan \sqrt{-\varepsilon_m / \varepsilon_d}} \tag{3}$$

where ε_m is the relative permittivity of the metal, ε_d is the relative permittivity of the dielectric material within the hole and l is the length of the long edge of the rectangle. At 750 nm, the real part of the dielectric constant for silver is –27.8, which leads to a 14% increase in cut-off wavelength for a 270 nm hole. Second, the coupling between SPs on the top and bottom edges inside the hole leads to an increased effective index.

Figure 2 shows the combination of these two effects for a TE_{01} mode in a real metal. The cut-off wavelength occurs when the effective index goes to zero. The effective index method (shown with curves) agrees well with rigorous electromagnetic simulations (shown with points). In the effective index method, the effective index squared equals ε_d in equation (3). Also shown is the cut-off wavelength for a PEC, which is significantly reduced from that of real metal. The calculations also agree well with experimental observations. Calculations were performed for hole-widths down to 15 nm, where cut-off wavelengths increased up to 1260 nm.

Figure 2 Effective index squared, calculated by the effective index method shown as continuous curves, verified by numerical simulations, shown as points, for the TE_{01} rectangular holes in silver. The lengths of the sides are indicated in the legend. Parameters were chosen to match published experimental results [17]. Reprinted with permission from [25]. Copyright 2005 The Optical Society of America (for colours see online version)

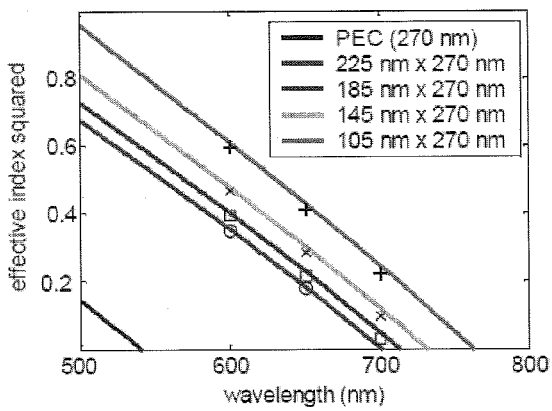

Figure 3 shows the distribution of electric and magnetic field components as calculated by finite difference computations. This figure shows clearly the influence of the SP modes in the z-component of the electric field at the top and bottom edges inside the hole in a silver film. It also shows the penetration of the field into the metal for the other components.

Figure 3 Electric (E) and magnetic (H) field components along the x, y and z directions for the TE_{01} mode in a 105 nm by 270 nm rectangular hole in silver, at a wavelength of 750 nm as calculated using the finite difference method. Reprinted with permission from [25]. Copyright 2005 The Optical Society of America

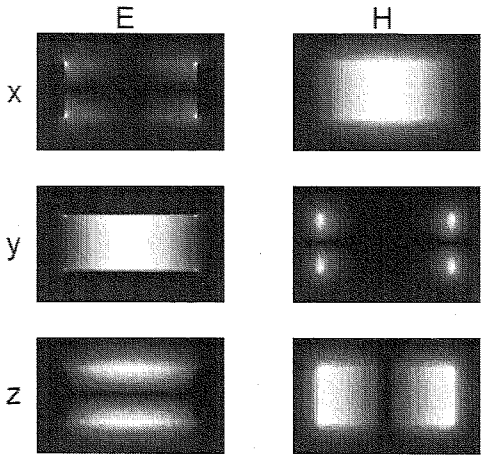

The origin of increased cut-off wavelength has been explained with the theoretical analysis presented here. We have shown the influence of LSPs on the wavelength for transmission through a sub-wavelength rectangular aperture in a real metal, through simulations and calculations. The origin of the peak in transmission or the resonance has not yet been explained. This will be dealt with in the next section.

2.2.2 Resonant light transmission through rectangular nano-holes

In the previous section, it was described how changes in the aspect ratio of a sub-wavelength rectangular aperture cause strong changes in the cut-off wavelength. Decreasing the short-edge length of the hole was found to increase the cut-off wavelength. The effect of the shape of the nano-hole is not limited to an increase in the cut-off wavelength. We demonstrated that there is also a Fabry-Pérot (FP) resonance, leading to a maximum in transmission close to the cut-off wavelength [26].

In a rectangular waveguide, there exists an impedance mismatch between the modes in the waveguide and the free space modes, which gives rise to reflections. For a PEC waveguide, it is found that there is a phase-shift associated with this reflection, and the reflection coefficient is given by [27,28]:

$$\Gamma = |r| \exp(j\varphi) = 0.25 \exp(j0.42\pi). \tag{4}$$

For a rectangular nano-hole in a real metal, such as silver, due to the presence of LSPs, the amplitude of the reflection coefficient is larger than expected. Therefore, the zeroth order FP resonance exists for film thickness smaller than half the wavelength of light.

Figure 4 shows the cut-off wavelength calculated for a 270 nm by 105 nm hole using the Drude model to calculate the dielectric constant for silver [29]. Figure 4(a) shows the effective index varying with wavelength, and also the fact that it reduces close to zero at the cut-off wavelength of 792 nm. It does not, however, actually become zero. This is due to the finite loss of the film. Figure 4(b) shows the loss of the lowest order mode as a

function of wavelength as calculated using the finite difference time domain (FDTD) method. A large attenuation is observed beyond cut-off wavelength.

Figure 4 (a) Plot of effective index as a function of wavelength and (b) loss in the film as a function of wavelength. Graphs are for a 270 nm by 105 nm hole in silver. Reprinted with permission from [26]. Copyright 2006 IEEE

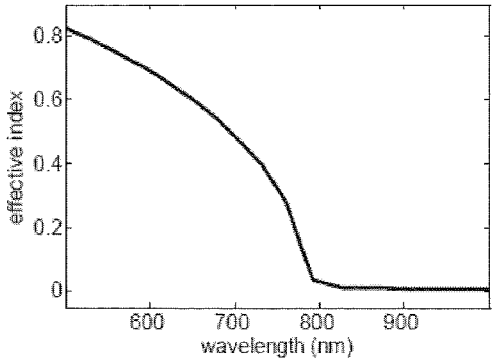

(a)

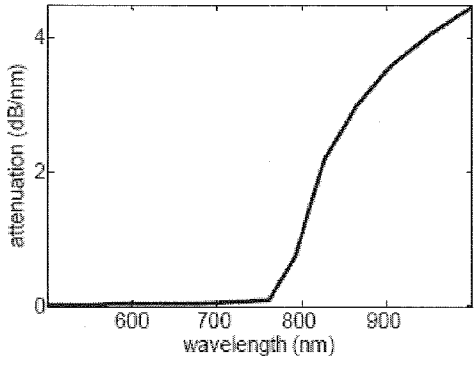

(b)

Figure 5 is a contour plot of transmission as a function of wavelength. The zeroth, first and second order FP resonances are shown as peaks in transmission. The zeroth order mode is found to exist at longer wavelengths, and for very thin films due to the negative phase of the reflection between the modes in the hole and free space.

The phase of reflection of the first order mode is calculated as [26]:

$$m\pi - \left(\frac{2\pi\eta_{\text{eff}}L}{\lambda}\right) = \varphi \tag{5}$$

where η_{eff} is the effective index obtained from a modal analysis of the rectangular metal waveguide structure. The phase shifts calculated using equation (5) and Figure 5 were found to increase with wavelength as silver becomes a better conductor, approaching the PEC case.

Figure 5 Contour plot of transmission as a function of wavelength. The cut-off wavelength, as calculated from Figure 4 is marked with a dashed line. Mode orders are marked $m = 0$, 1 and 2. Reprinted with permission from [26]. Copyright 2006 IEEE

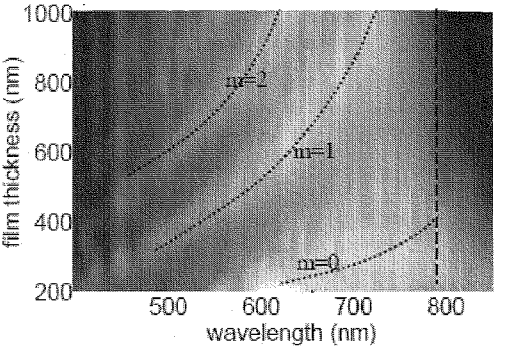

The increased cut-off wavelength and the peak in the light transmission through a single rectangular sub-wavelength aperture in a real metal were explained in this section. The effect of the aspect ratio of the hole on the coupling between SP modes allows for an increase in the effective dielectric leading to a significant red shift in the cut-off condition. Also, the existence of a Fabry-Pérot resonance close to cut-off wavelength was demonstrated using FDTD simulations.

2.3 Basis and lattice polarisation mechanisms

Based on the above results, it is clear that the shape the nano-hole has an important effect on the properties of the optical transmission. However, it would be incorrect to consider that this is the only factor influencing transmission for arrays of nano-holes. Indeed, we demonstrated experimentally that the orientation of the nano-holes within the array also plays a key role in the transmission [16]. The optical behaviour of elliptical holes was compared to that of double circular holes to clearly separate the effects of the lattice and the basis.

Figure 6 shows our experiments and theory to explain the separate contributions of the basis and the lattice. Figure 6(a) shows the elliptical and double-holes that were fabricated on a 100 nm thick gold film. Figure 6(b) shows the observed maximum transmission intensity for the (0, 1) SP resonance (left axis) and the polarisation angle (right axis) as a function of basis angle. Figure 6(c) shows the transmission intensity and polarisation angle for ellipses and double-holes as calculated by the FDTD method.

The ellipses exhibited maximum transmission when the light was polarised perpendicular to the major axis and on rotation, polarisation followed the basis and not the lattice vector. The double-holes, on the other hand, exhibited maximum transmission when light was polarised along the [1, 0] lattice direction for all angles, and the polarisation followed the lattice and not the basis. The maximum transmission for ellipses was constant, in spite of the changes in the basis orientation. The maximum intensity for the double-holes decreased with increase in the basis angle.

Figure 6 (a) Scanning electron microscope images of elliptical and double-holes with different basis orientations. The lattice directions are also defined; (b) maximum transmission intensity and polarisation angle as a function of basis angle and (c) FDTD calculated transmission and polarisation angle. Solid lines show maximum intensity for ellipses (open squares), and double-holes (open circles). Dashed lines show polarisation angle for ellipses (filled squares) and double-holes (filled circles). Reprinted with permission from [16]. Copyright 2005 American Chemical Society

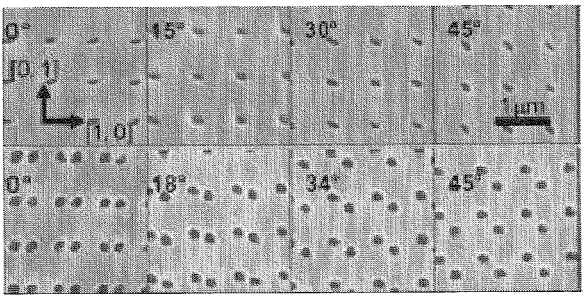

(a)

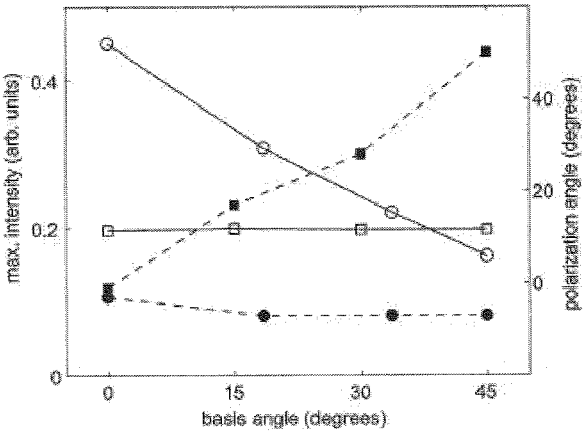

(b)

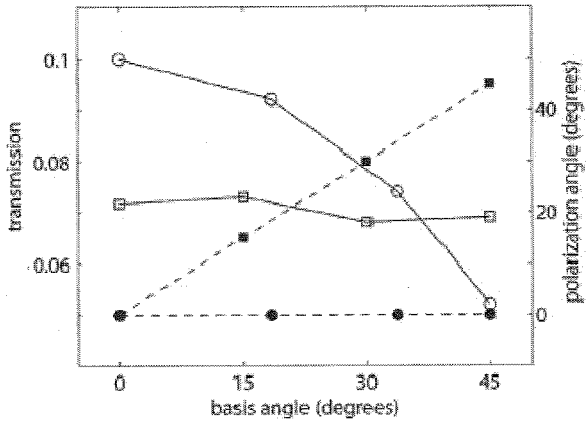

(c)

Two separated mechanisms are at play in determining the observed polarisation dependence. First, when light hits the surface it is scattered by the holes into the surface waves. The direction and polarisation of this scattering depends upon the orientation of the holes. The maximum scattering occurs for polarisation perpendicular to the long-axis of both the double-holes and the ellipses. In this sense, both of these bases show the same behaviour upon rotation.

Second, each individual basis influences the polarisation of light that is transmitted through the holes. While the elliptical holes have a strong polarisation dependence on the transmission, the double-holes are almost polarisation independent because they are essentially two isolated circular holes. Therefore, this second mechanism of transmission is different for the double-holes and ellipses.

These observations indicate that lattice and basis contribute separately to the transmission properties of shaped nano-holes. These were the first experiments to show that when designing nano-hole arrays to optimise the optical properties for a specific application, both the basis and the lattice should be considered. Indeed, the basis and the lattice provide two degrees of freedom for maximising the performance of nano-photonic devices based on this kind of substrate.

3 The double-hole: apexes for sub-wavelength focusing

Sub-wavelength hole arrays can enhance the optical transmission, and by changing the shape and orientation of the nano-holes it is possible to tailor their optical properties. Many applications require local field enhancements, rather than increased transmission. These applications include SERS, SHG and other forms of non-linear optics. We have demonstrated, both theoretically and experimentally, the capability of overlapping double-holes to provide the required field enhancements for those applications [21,23].

Part of our motivation to study double-holes was that they are easy to fabricate. Two isolated holes may be readily created by FIB milling, and precisely made to overlap by changing the displacement between them. The field enhancement in the double-hole structure comes from the apexes formed where the double-holes overlap. The apex-gap that is formed is analogous to the gap found in bowtie antennae [30], optical antennae [31], which are other structures that have been used to demonstrate strong local field enhancements. We studied the changes on the transmission and local field enhancement properties for double-holes of varying separation, from two isolated holes to their merging as a single hole.

3.1 Transmission through double-holes: theory and experiment

To characterise the optical properties, we performed FDTD simulations for the double-hole structure for six different hole separations [21]. The hole-separations were 0, 90, 130, 190 and 250 nm. The diameter of each of the holes was 200 nm. The first and last structures represent single-holes and completely separated double-holes respectively. All other structures are overlapping double-holes with different apex gaps.

Figure 7 shows the normalised peak transmission for the six structures as calculated using the FDTD method. The highest transmission is observed in the double-hole structure with the hole separation of 190 nm. This structure has an apex gap

of 65 nm. The transmission for the separated double-hole was seen to decrease to a value close to that of a single-hole.

Figure 7 Transmission spectra of various double-hole structures as a function of hole separation as calculated by the FDTD method. Reprinted with permission from [21]. Copyright 2006 Springer

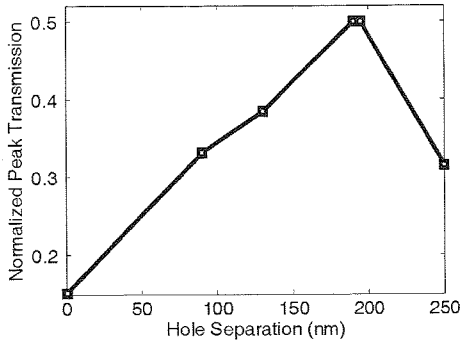

We performed transmission measurements on arrays of overlapping double-holes. The arrays were fabricated to match the structures used for finite difference calculations. We found that the first and last arrays (the single hole and separated double-holes) exhibited transmission characteristics similar to past experiments [1,16]. Entirely different behaviour was exhibited by the arrays where apexes were present. The transmission peak was enhanced and red-shifted by a factor or 30 nm for the 195 nm array.

Figure 8 shows the measured normalised peak intensity for the different hole separations. The intensity increases until the point where the holes are no longer touching, and drops abruptly from there on.

Figure 8 Measured normalised peak transmission as a function of hole separation. The diagrams of the double-holes illustrate hole separation. Reprinted with permission from [21]. Copyright 2006 Springer

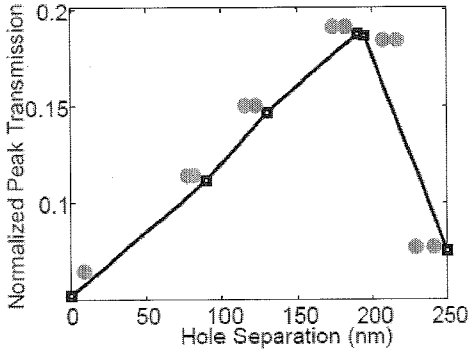

It was observed that the closest apex gap of 35 nm did not yield maximum transmission. The 190 nm and 195 nm arrays exhibited similar transmission values, but the array with 65 nm apex gap had a higher transmission. This agreed well with the results we obtained from FDTD computations.

The values of normalised transmission obtained from calculations were higher than experimental values. This is because of sharper apexes in the simulated structures, although the trend observed is the same. This shows that there is good correspondence between the structures fabricated and the theory, even though imperfections exist from the fabrication process.

3.2 SHG from double-hole apex structures

We have established both theoretically and experimentally that overlapping double-holes exhibit enhanced transmission higher than single-holes. Next, we went on to investigate the local field intensity in the apex gap. This is important to non-linear applications like SHG because the efficiency of SHG is proportional to the square of the local field intensity. We found an enhancement in SHG from the overlapping double-hole structure. Theoretical calculations demonstrated an increased local field intensity, which corroborates the experimental findings [23].

Within the dipole approximation, SHG is not possible for centro-symmetric materials like bulk gold, but may be observed on the surface where the symmetry is broken, and rough surfaces exhibit enhanced SHG [32]. The double-hole structure with apexes is thus particularly useful for SHG because it allows for optical focusing and hence, enhanced field at the apexes.

SHG enhancement in a number of double-hole arrays was measured. The array periodicity was kept constant, and the hole spacing was varied between 90 nm (single hole) and 250 nm (two separated holes). The apexes were the sharpest for 220 nm hole spacing. Enhanced SHG was found to depend on the incident light polarisation and the hole spacing.

Figure 9 shows the measured SHG plotted against hole spacing. The SHG intensity was found to depend strongly on polarisation, as is apparent from the graph. The x-polarisation was defined as parallel to the major axis of the double-hole structure, and the y-polarisation was defined as perpendicular to the major axis of the double-hole structure. The x-polarisation is equivalent to the s-polarisation defined for the elliptical holes, and the y-polarisation is equivalent to the p-polarisation.

Figure 9 SHG vs. hole spacing, for x- and y- polarisations. Reprinted with permission from [23]. Copyright 2006 American Institute of Physics

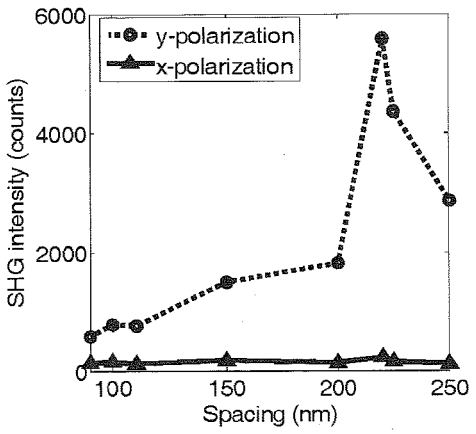

From the graph, a strong peak in the SHG can be seen for hole spacing of 220 nm. The intensity (5600 counts) is enhanced ten times with respect to the 90 nm hole spacing value. This enhancement was found to be of the order of 1.5 times for linear transmission measurements. Considering the squared dependence of SHG on intensity, an enhancement of only 2.25 would be expected. This showed that an additional enhancement of 4.44 times was present.

Figure 10 shows the *y*-polarised electric field, calculated by finite difference method, 5 nm above the gold surface, shown on a log scale. The maximum field intensity increases by four times between the apexes, giving a net enhancement factor of 16. This is localised in the small area near the apexes. This is in agreement to the enhancements observed in SHG from the structure.

Figure 10 FDTD calculated electric field for 220 nm hole, shown on a log scale. Reprinted with permission from [23]. Copyright 2006 American Institute of Physics

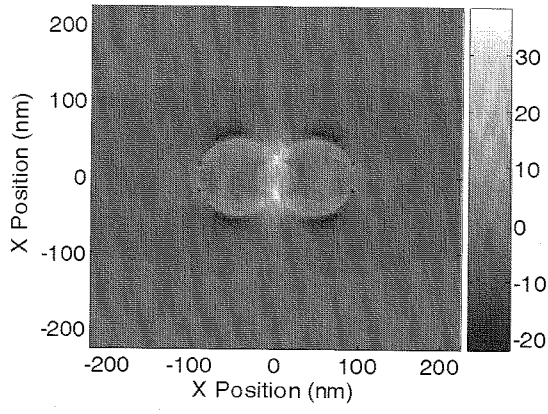

These findings indicate that the presence of sharp apexes can enhance local field intensity. This makes the overlapping double-hole structure useful for non-linear applications. We are currently exploring the use of this structure in other spectroscopic applications like SERS.

4 Nano-holes for spectroscopy

Enhanced spectroscopic methods, such as SERS and surface enhanced fluorescence spectroscopy (SEFS), are very useful in chemical analysis. These methods allow the detection of extremely small amounts of adsorbed species, even achieving the ultimate sensitivity at the single molecule level [33]. As demonstrated in the previous sections, the enhancement in the field intensity resulting from sub-wavelength apertures can be tailored by optimising their fabrication parameters, such as shape, film thickness and periodicity. We found that arrays of circular nano-holes can be used as substrates for enhanced Raman scattering and enhanced luminescence. The properties of the arrays were varied to find the conditions for maximum enhancement and sensitivity [34–36].

4.1 Enhanced Raman scattering

We demonstrated that sub-wavelength arrays on 100 nm gold films can be used as substrates for enhanced Raman scattering [34]. In these experiments, a probe dye molecule was adsorbed onto the array of nano-holes and the excitation laser was directed through the back of the substrate. Therefore, the excitation laser needed to go through the nano-holes to excite the molecules adsorbed on the gold surface and the scattering was measured in a forward geometry.

Numerical calculations showed that the electric field from periodic arrays of circular holes is localised within the holes and at the rims of the holes [35]. Only molecules subjected to the enhanced local electromagnetic field contributed to the measured SERS signal. Therefore, it is expected that the SERS is coming mainly from molecules inside the holes.

Figure 11 shows the enhanced Raman spectra from 10 μM of oxazine 720 dye in methanol adsorbed on nano-hole arrays of three different periodicities fabricated on a gold film. It is clear from Figure 11 that the enhancement factor is dictated by the array periodicity. The maximum enhancement being observed for the array (a) in Figure 11, which exhibited maximum transmission at the excitation laser wavelength.

Figure 11 Enhanced Raman scattering from oxazine 720 adsorbed on nano-hole arrays with periodicities: (a) 560 nm; (b) 590 nm and (c) 620 nm. The spectra are offset for clarity. Reprinted with permission from [34]. Copyright 2004 American Chemical Society

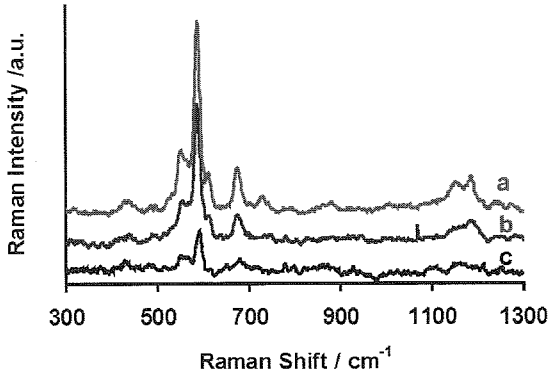

For this experimental geometry, when the laser wavelength coincides with the surface plasmon resonance, enhanced transmission for normal incidence is observed. Hence, an increase in the number of laser photons reaching the gold-air interface is expected under resonance conditions. This allows for a localised enhanced field at the surface. The enhanced local field is required for any surface-enhanced spectroscopic method; therefore, the strongest Raman signal is expected for the array that has enhanced transmission closest to the laser wavelength. This is in agreement with the experimental results.

Similar experiments were performed with other organic molecules, but a clear enhanced scattering was only observed for adsorbed species that have internal resonances within the laser frequency [34]. This seems to imply that a resonance Raman effect was also contributing to the overall enhancement.

4.2 Enhanced fluorescence

The enhanced transmission and local field intensity of sub-wavelength apertures in a metal film can be used to excite a fluorescent material adsorbed on the surface. We demonstrated that higher fluorescence sensitivities are achieved when fluorescence spectroscopy measurements are performed on sub-wavelength hole arrays [36]. Several nano-hole arrays with different periodicities were spin-coated with polystyrene (PS) doped with varying concentrations of Oxazine 720 fluorescent dye. Again, the excitation laser was directed at the back of the substrate and the extraordinary transmission of light through the nano-holes led to the dye being excited. Enhanced fluorescence, and consequently, high fluorescence sensitivities were observed at SPR conditions.

Figure 12 shows the measured fluorescence enhancement as a function of periodicity. Seven different square arrays of circular holes with 100 nm diameter and different periodicities were fabricated. The fluorescence spectra obtained indicated quite clearly that the fluorescence efficiency was array dependent. The highest fluorescence intensity was obtained for the 553 nm array, which was the array that exhibited maximum enhanced transmission at the laser wavelength. The enhancement factor was found to be 82. We found that the relation between integrated florescence and transmission is non-linear. This could be due to secondary enhancement from oxazine emission.

Figure 12 Enhancement factor for arrays of nano-holes of different periodicities. Arrays were coated with a PS film doped with 9.6 μM of oxazine 720. Reprinted with permission from [36]. Copyright 2005 American Chemical Society

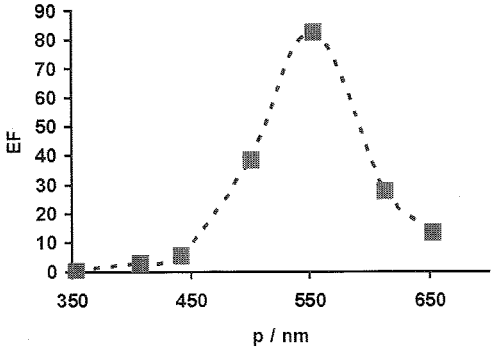

4.3 Quantum dots

The coupling of the emission from semiconducting quantum dots (QD) to SPPs has been explored for several different metallic nanostructures [37,38]. One of the main effects observed is the quenching of the QD photoluminescence (PL) into SP modes. Nano-holes arrays on a metal surface can efficiently transform SPPs into free photons, and thus should increase the PL efficiency from adsorbed QDs. We demonstrated this effect for the first time, and observed an enhancement in spontaneous emission by two orders of magnitude [39] for QDs adsorbed on nano-hole arrays. The wavelength at which maximum PL emission occurs can be tuned by altering the geometric characteristics of the arrays.

We used nine nano-hole arrays of different periodicities and diameters. Films of polystyrene-block-poly(acrylic acid) copolymer (PS-b-PAA)-stabilised cadmium

sulphide (CdS) QDs were used to coat the substrate. CdS was selected because trap state emission from these QDs (610 nm) overlaps with the SP resonances of the nano-holes used. A solution of the copolymer-stabilised CdS quantum dots (designated PS-QD) was drop-coated on the various gold arrays. Transmission and PL measurements were carried out for these samples. In order to have a baseline, measurements were performed on a glass slide coated with PS-QD, without the gold layer.

Figure 13 shows the PL decay curves of PS-QD films, on a glass slide and adsorbed on nano-hole arrays on gold film. The average lifetimes measured from Figure 13 were 282 and 31 ns for the PS-QD films coated on glass and the nano-hole arrays, respectively. The significant decrease in the PL lifetime for the PS-QD film on the array of nano-holes can be attributed by the quenching of the spontaneous emission into the SP modes of the nanostructure. The main contribution to the multi-exponential decay for the PS-QD film adsorbed on glass was from the component at 360 ns, consistent with CdS trap state emission. On the other hand, the main component for the PS-QD on the nano-hole array was at 5 ns. This implies that a Purcell factor of 72 can be calculated from the ratio of the main decay components.

Figure 13 PL decay curves for PS-QD film on (a) glass substrate and (b) adsorbed on nanohole array of 550 nm periodicity, with hole diameter equal to 122 nm. Reprinted with permission from [39]. Copyright 2006 American Chemical Society

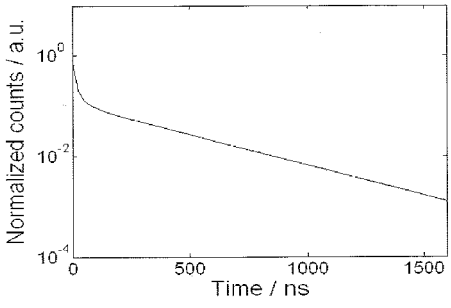

(a)

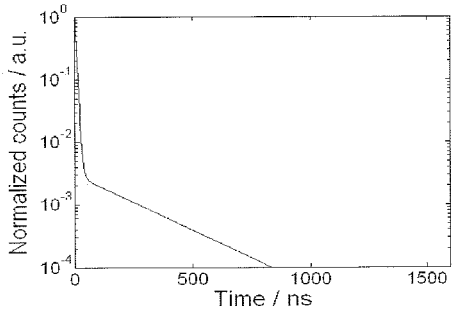

(b)

The PL spectra transmitted through the arrays were significantly different than the one observed from the glass substrate. Moreover, the PL spectrum of each array matched its white light transmission spectrum. This indicates that the emission characteristics of the PS-QD are readily modified by the plasmonic states supported by the nanostructures.

PL enhancement was also observed for each of the arrays. The enhancement factor was calculated as follows:

$$F = \frac{T_{PL}}{T_{WL}} \tag{6}$$

where T_{PL} is the integrated PL transmittance through the arrays and T_{WL} is the total transmittance of white light through the PS-QD coated arrays [36].

The enhancement factor varied from nearly 40 to 300. Observations indicated that maximum enhancement occurred for arrays designed to produce best overlap between SPR and PL emission.

5 Nano-holes for sensing

The enhanced optical properties of sub-wavelength apertures have been attributed to diffractive mechanisms [10–12]. Our work [25,26] proved that LSP do play an important role in enhancing transmission. Both mechanisms indicate that the enhanced transmission through nano-hole arrays depends on the optical properties at the gold-dielectric interface. This is the basis for chemical sensors that can be used to monitor surface events very effectively.

We used nano-holes fabricated on a metal film to develop a transmission based SPR sensor [40], and further integrate this sensing element into a microfluidic prototype device [41].

5.1 SPR sensors

Most SPR sensors that are commercially available operate based on total internal reflection using what is known as the Kretschmann configuration [42]. The SPR sensor based on arrays of nano-holes operates based on transmission rather than reflection [40]. This is useful because the transmitted and measured signals are collinear. The setup is therefore easier to align. Also, when nano-holes are used for sensor applications, the resulting localisation of the analyte can directly benefit from the local field intensities and optical properties of nano-holes, thus making nano-hole sensors useful.

A sensor based on arrays of nano-holes on a gold film was used to monitor binding of organic and biological molecules [40]. Several arrays of different periodicities with hole diameter of 200 nm were fabricated. The slides were immersed in a 1 mM ethanoic solution of 11-mercaptoundecanoic acid (MUA) for a period of 24 h. The surface was then dried, and the normal transmission spectra were measured. The surface was then further modified by bovine serum albumin (BSA) which adsorbed on top of the MUA monolayer.

Figure 14 shows the normalised transmission spectra of normally incident white light though one of the arrays of nano-holes. The transmission spectrum through the array of nano-holes prior to the surface modifications shows a sharp resonance at 645 nm. After surface treatment with MUA, the same array showed a shift in maximum transmission to 650 nm. An additional shift to 654 nm was observed after the BSA protein was adsorbed on the MUA surface.

Figure 14 Transmission spectra of normally incident white light through nano-hole array. (a) Clean gold surface; (b) gold modified with a monolayer of MUA and (c) gold-MUA modified with albumin. Reprinted with permission from [40]. Copyright 2004 American Chemical Society

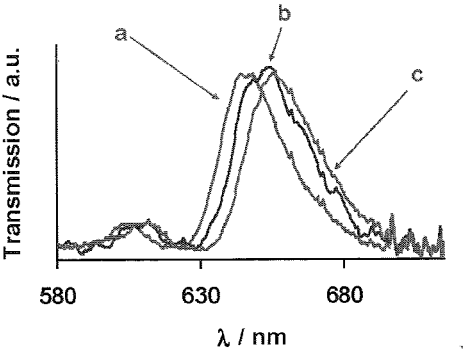

Since this sensor uses transmission, alignment is simpler when compared to the Kretschmann arrangement, because incident and detected signals are collinear. However, sensors operating in the Kretschmann configuration are known to exhibit better sensitivities.

5.2 Microfluidic integration

Microfluidic devices enable the manipulation of the small quantities of chemicals generally used in biomedical analyses. So-called lab-on-chip or micro total analysis systems promise increased quality and quantity of analytical tests, with decreased time and cost requirements [43]. Microfluidic channels have been used in conjunction both with nano-cavity arrays for bio-sensing [44], and nano-hole arrays for studying the effect of refractive index of the fluid on resonant transmission [45].

We recently demonstrated nano-hole based detection within a microfluidic chip framework [41]. Figure 15 shows a schematic representation of the SPR sensor chip.

Figure 15 Schematic representation of microfluidic SPR sensor chip [41]

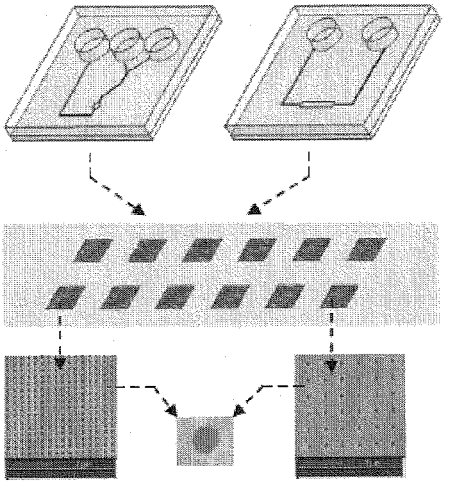

A number of nano-hole arrays, 20×20 μm, with hole diameter 100 nm and different periodicities were fabricated on a gold film. Microfluidic channels were constructed by soft lithographic methods, and aligned over the sensor array substrate. The two microfluidic configurations enabled single solution experiments over multiple arrays as well as the generation of concentration gradients across a set of similar arrays. Glucose solutions of known refractive index were used to determine the sensitivity, 333 nm/RIU (refractive index unit). Employing the set of nanohole arrays, the device was applied to detect microfluidic concentration gradients as well as surface binding during the assembly of cysteamine monolayer-biotin-streptavidin surface groups.

Our measurements indicate that multiple arrays of nanoholes, differentiated by periodicity, may be integrated and used as SPR chemical/biological detectors in a microfluidic chip format. Combining the unique optical properties of nano-hole arrays with microfluidic processing and control presents several opportunities in bio-sensing that are being currently explored by our group.

6 Conclusions

The unique optical properties of sub-wavelength apertures have spurred considerable research interest over the past few years. This is mainly due to two factors: novel transmission properties, and more recently, enhanced local field properties within the holes. By virtue of these properties, nano-holes in metal films are proving to be very useful for applications in spectroscopy and sensing. Creating new structures for enhancing transmission and local field, developing novel applications, devising cheaper and easier techniques for fabricating nano-holes, and further characterisation of existing structures are subjects of current work in this area.

Research in sub-wavelength optics is burgeoning. Several experiments and proof-of-concept applications, such as the ones described in this review, indicate that these structures may play a central role in a new generation of plasmonic devices.

Acknowledgements

We gratefully acknowledge funding support for this work from NSERC, CFI and BCKDF. This collaboration has also been facilitated by the Centre for Advanced Materials and Related Technology (CAMTEC) at the University of Victoria and the Pacific Centre for Advanced Materials and Microstructures (PCAMM).

References

1 Ebbesen, T.W., Lezec, H.J., Ghaemi, H.F., Thio, T. and Wolff, P.A. (1998) 'Extraordinary optical transmission through sub-wavelength hole arrays', *Nature*, Vol. 391, No. 12, pp.667–669.

2 Grupp, D.E., Lezec, H.J., Thio, T. and Ebbesen, T.W. (1999) 'Beyond the Bethe limit: tunable enhanced light transmission through a single sub-wavelength aperture', *Adv. Mater.*, Vol. 11, No. 10, pp.860–862.

3 DiMaio, J.R. and Ballato, J. (2006) 'Polarization dependant transmission through subwavelength anisotropic aperture arrays', *Opt. Express*, Vol. 14, No. 6, pp.2380–2384.

4 Moskovits, M. (1985) 'Surface enhanced spectroscopy', *Rev. Mod. Phys.*, Vol. 57, No. 3, pp.783–828.

5 Hecht, B., Sick, B., Wild, U.P., Deckert, V., Zenobi, R., Martin, O.J.F. and Pohl, D.W. (2000) 'Scanning near field optical microscopy with aperture probes: fundamentals and applications', *J. Chem. Phys.*, Vol. 112, No. 18, pp.7761–7774.

6 Airola, M. and Blair, S. (2005) 'Second harmonic generation from an array of sub-wavelength metal apertures', *J. Optics A: Pure and Appl. Opt.*, Vol. 7, pp.118–123.

7 Baida, F.I., van Labeke, D. and Guizal, B. (2003) 'Enhanced confined light transmission by single subwavelength apertures in metallic films', *Appl. Opt.*, Vol. 42, No. 34, pp.6811–6815.

8 Raether, H. (1988) *Surface Plasmon*, Springer-Verlag, Berlin.

9 Ghaemi, H.F., Thio, T., Grupp, D.E., Lezec, H.J., Ebbesen, T.W. and Lezec, H.J. (1998) 'Surface-plasmons enhance optical transmission through subwavelength holes', *Phys. Rev. B*, Vol. 58, No. 11, pp.6779–6782.

10 Treacy, M.M.J. (2002) 'Dynamical diffraction explanation of the anomalous transmission of light through metal gratings', *Phys. Rev. B*, Vol. 66, Article 195105.

11 Cao, Q. and Lalanne, P. (2002) 'Negative role of surface plasmons in the transmission of metallic gratings with very narrow slits', *Phys. Rev. Lett.*, Vol. 88, No. 5, Article 057403.

12 Lezec, H.J. and Thio, T. (2004) 'Diffracted evanescent wave model for enhanced and suppressed optical transmission through subwavelength hole arrays', *Opt. Express*, Vol. 12, No. 16, pp.3629–3651.

13 Gordon, R., Brolo, A.G., Mc Kinnon, A., Rajora, A., Leathem, B. and Kavanagh, K.L. (2004) 'Strong polarization in the optical transmission through elliptical nano-hole arrays', *Phys. Rev. Lett.*, Vol. 92, No. 3, Article 037401.

14 van der Molen, K.L., Koerkamp, K.J.K., Enoch, S., Segerink, F.B., van Hulst, N.F. and Kuipers, K.L. (2005) 'Role of shape and localized resonances in extraordinary transmission through periodic arrays of subwavelength holes: experiment and theory', *Phys. Rev. B*, Vol. 72, Article 045421.

15 Koerkamp, K.J.K., Enoch, S., Segerink, F.B., van Hulst, N.F. and Kuipers, K.L. (2004) 'Strong influence of hole shape on extraordinary transmission through periodic arrays of subwavelength holes', *Phys. Rev. Lett.*, Vol. 92, No. 18, Article 183901.

16 Gordon, R., Hughes, M., Leathem, B., Kavanagh, K.L. and Brolo, A.G. (2005) 'Basis and lattice polarization mechanisms for light transmission through nano-hole arrays in a metal film', *Nano Lett.*, Vol. 5, No. 7, pp.1243–1246.

17 Degiron, A., Lezec, H.J., Yamamoto, N. and Ebbesen, T.W. (2004) 'Optical transmission properties of a single subwavelength aperture in a real metal', *Opt. Commun.*, Vol. 239, Nos. 1–3, pp.61–66.

18 Wenger, J., Lenne, P.F., Popov, E., Rigneault, H., Dintinger, J. and Ebbesen, T.W. (2005) 'Single molecule fluorescence in rectangular nano-apertures', *Opt. Express*, Vol. 13, No. 18, pp.7035–7044.

19 Rigneault, H., Capoulade, J., Dintinger, J, Wenger, J., Bonod, N., Popov, E., Ebbesen, T.W. and Lenne, P-F. (2005) 'Enhancement of single molecule fluorescence detection in subwavelength apertures', *Phys. Rev. Lett.*, Vol. 95, Article 117401.

20 Liu, Y. and Blair, S. (2003) 'Fluorescence enhancement from an array of subwavelength apertures', *Opt. Lett.*, Vol. 28, No. 7, pp.507–509.

21 Kumar, L.K.S., Lesuffleur, A., Hughes, M.C. and Gordon, R. (2006) 'Double nano-hole apex – enhanced transmission in metal films', *Appl. Phys. B*, Vol. 84, pp.25–28.

22 Homola, J., Yee, S.S. and Gauglitz, G. (1999) 'Surface plasmon resonance sensors: review', *Sens. Actuators, B*, Vol. 54, pp.3–15.

23 Lesuffleur, A., Kumar, L.K.S. and Gordon, R. (2006) 'Enhanced second harmonic generation from nanoscale double-hole arrays in a gold film', *Appl. Phys. Lett.*, Vol. 88, p.261104.

24 Martìn-Moreno, L., Garcìa-Vidal, F.J., Lezec, H.J., Pellerin, K.M., Thio, T., Pendry, J.B. and Ebbesen, T.W. (2001) 'Theory of extraordinary optical transmission through subwavelength hole arrays', *Phys. Rev. Lett.*, Vol. 86, No. 6, pp.1114–1117.

25 Gordon, R. and Brolo, A.G. (2005) 'Increased cut-off wavelength for a subwavelength hole in a real metal', *Opt. Express*, Vol. 13, No. 6, pp.1933–1938.

26 Gordon, R., Kumar, L.K.S. and Brolo, A.G. (2006) 'Resonant light transmission through a nano-hole in a metal film', *IEEE Trans. Nanotechnol.*, Vol. 5, No. 3, pp.291–294.

27 Croswell, W.F., Rudduck, R.C. and Hatcher, D.M. (1967) 'The admittance of a rectangular waveguide radiating into a dielectric slab', *IEEE Trans. Antennas Propogat.*, Vol. 15, No. 5, pp.627–633.

28 MacPhie, R.H. and Zaghloul, A.I. (1980) 'Radiation from a rectangular waveguide with infinite flange- exact solution by the correlation matrix method', *IEEE Trans. Antennas Propogat.*, Vol. 28, No. 4, pp.497–503.

29 Johnson, P.B. and Christy, R.W. (1972) 'Optical constants of noble metals', *Phys. Rev. B: Condens. Matter*, Vol. 6, No. 12, pp.4370–4379.

30 Schuck, P.J., Fromm, D.P., Sundaramurthy, A., Kino, G.S. and Moerner, W.E. (2005) 'Improving the mismatch between light and nanoscale objects with gold bowtie nanoantennas', *Phys. Rev. Lett.*, Vol. 94, Article 017402.

31 Stockman, M.I. (2004) 'Nanofocusing of optical energy in tapered plasmonic waveguides', *Phys. Rev. Lett.*, Vol. 93, No. 13, Article 137404.

32 Chen, C.K., de Catsro, A.R.B. and Shen, Y.R. (1981) 'Surface- enhanced second harmonic generation', *Phys. Rev. Lett.*, Vol. 46, No. 2, pp.145–148.

33 Kneipp, K., Kneipp, H., Itzkan, I., Dasari, R.R. and Feld, M.S. (1999) 'Ultrasensitive chemical analysis by Raman spectroscopy', *Chem. Rev.*, Vol. 99, No. 10, pp.2957–2976.

34 Brolo, A.G., Arctander, E., Gordon, R., Leathem, B. and Kavanagh, K.L. (2004) 'Nano-hole-Enhanced Raman scattering', *Nano Lett.*, Vol. 4, No. 10, pp.2015–2018.

35 Krishnan, A., Thio, T., Kim, T.J., Lezec, H.J., Ebbesen, T.W., Wolff, P.A., Pendry, J., Martin-Moreno, L. and Gracia-Vidal, F.J. (2001) 'Evanescently coupled resonance in surface plasmon enhanced transmission', *Opt. Commun.*, Vol. 200, pp.1–7.

36 Brolo, A.G., Kwok, S.C., Moffitt, M.G., Gordon, R., Riordon, J. and Kavanagh, K.L. (2005) 'Enhanced fluorescence from arrays of nano-holes in a gold film', *J. Am. Chem. Soc.*, Vol. 127, pp.14936–14941.

37 Kulakovich, O., Strekal, N., Yaroshevic, A., Maskevich, S., Gaponenko, S., Nabiev, I., Woggon, U. and Artemyev, M. (2002) 'Enhanced luminescence of CdSe quantum dots on gold colloids', *Nano Lett.*, Vol. 2, No. 12, pp.1449–1452.

38 Shimizu, K.T., Woo, W.K., Fisher, B.R., Eisler, H.J. and Bawendi, M.G. (2002) 'Surface enhanced emission from single semiconductor nanocrystals', *Phys. Rev. Lett.*, Vol. 89, Article 117401.

39 Brolo, A.G., Kwok, S.C., Cooper, M.D., Moffitt, M.G., Wang, C.W., Gordon, R., Riordon, J. and Kavanagh, K.L. (2006) 'Surface plasmon- Quantum dot coupling from arrays of nano-holes', *J. Phys. Chem.*, Vol. 110, pp.8307–8313.

40 Brolo, A.G., Gordon, R., Leathem, B. and Kavanagh, K.L. (2004) 'Surface plasmon sensor based on the enhanced light transmission through arrays of nano-holes in gold films', *Langmuir*, Vol. 20, pp.4813–4815.

41 de Leebeeck, A., Kumar, L.K.S., de Lange, V., Sinton, D., Gordon, R. and Brolo, A.G. (2007) 'On-chip surface-based detection with nano-hole arrays', *Anal. Chem.*, Vol. 79, pp.4094–4100.

42 Nice, E.C. and Catimel, B. (1999) 'Instrumental biosensors: new perspectives for the analysis of biomolecular interactions', *BioEssays*, Vol. 21, No. 4, pp.339–352.

43 Dittrich, P.S., Tachikawa, K. and Manz, A. (2006) 'Micro total analysis systems. Latest advancements and trends', *Anal. Chem.*, Vol. 78, pp.3887–3908.

44 Liu, Y., Bishop, J., Williams, L., Blair, S. and Herron, J. (2004) 'Biosensing based upon molecular confinement in metallic nanocavity arrays', *Nanotechnology*, Vol. 15, pp.1368–1374.

45 Tetz, K.A., Pang, L. and Fainman, Y. (2006) 'High-resolution surface plasmon resonance sensor based on linewidth-optimized nanohole array transmittance', *Opt. Lett.*, Vol. 31, No. 10, pp.1528–1530.